Thermodynamic Effects of Mutations on the Denaturation of T4 Lysozyme*

John H. Carra,* Elizabeth C. Murphy,# and Peter L. Privalov*
*Department of Biology and Biocalorimetry Center, The Johns Hopkins University, Baltimore, Maryland 21218, and #National Institutes of Health, National Institute of Arthritis, Diabetes, and Digestive and Kidney Diseases, Laboratory of Chemical Physics, Bethesda, Maryland 20892 USA

ABSTRACT We investigated the folding of substantially destabilized mutant forms of T4 lysozyme using differential scanning calorimetry and circular dichroism measurements. Three mutations in an α-helix in the protein's N-terminal region, the alanine insertion mutations S44[A] and K48[A], and the substitution A42K had previously been observed to result in unexpectedly low apparent enthalpy changes of melting, compared to a pseudo-wild-type reference protein. The pseudo-wild-type reference protein thermally unfolds in an essentially two-state manner. However, we found that the unfolding of the three mutant proteins has a reduced cooperativity, which partially explains their lower apparent enthalpy changes. A three-state unfolding model including a discrete intermediate is necessary to describe the melting of the mutant proteins. The reduction in cooperativity must be considered for accurate calculation of the energy changes of folding. Unfolding in two stages reflects the underlying two-subdomain structure of the lysozyme protein family.

INTRODUCTION

Small globular proteins (<15,000 MW) are generally found to unfold cooperatively (Privalov, 1979) in a single transition between a folded native state and a disordered denatured state. Such proteins can therefore be said to constitute a single domain, or cooperative unit of folding. Larger proteins are often found to unfold in multiple stages, which can be assigned to the denaturation of individual domains (Privalov, 1982). In some cases, the definition of domains can be made difficult by the presence of interacting units of substructure. If these subdomains have comparable stabilities, and their interaction is strong enough, they may fold together in a single cooperative process. Bilobite proteins such as the lysozymes and α-lactalbumin, or other proteins divided by an active site cleft, such as staphylococcal nuclease, fall into this category (Griko et al., 1995).

However, variation of solution conditions such as pH, or changes in amino acid sequence may sufficiently alter the relative stabilities of subdomains that they are no longer a single unit of folding. Our previously published results on staphylococcal nuclease (Carra et al., 1994a,c; Carra and Privalov, 1995) showed that many mutations of that protein result in changes in the cooperativity of folding, because of alterations of the relative stability of subdomains.

Determination of the degree of cooperativity in protein stability studies is crucially important, because the calculation of energetic parameters such as ΔH and ΔG can strongly depend on whether a two-state or multiple-state model is applied (Carra and Privalov, 1996). When mutations result in large changes in the apparent, or van't Hoff, enthalpy change of unfolding relative to a wild-type reference, as has often been found (Sturtevant, 1994), this suggests that the cooperativity of folding may have been affected. The exact degree of cooperativity of protein folding can be tested rigorously using differential scanning calorimetry (Privalov, 1979). Even when unfolding appears as a single transition using other techniques, there may actually be overlapping processes that are not discriminated. By detailed thermodynamic analysis of calorimetric data, one can determine the individual components of a complex process.

Heinz et al. (1993, 1994) had used circular dichroism to measure the stabilities of the three mutant T4 lysozyme proteins at pH 5.4 and found that their apparent enthalpy changes (ΔH_{app}) were anomalously low, indicating probable departure from two-state behavior. Our studies, at pH 3.0–4.0, confirm the non-two-state behavior and show the presence of an intermediate state in folding, which may represent a folded subdomain of the protein.

The structure of T4 lysozyme (Fig. 1) has an N-terminal lobe and a larger C-terminal lobe, linked by a long α-helix (Bell et al., 1991). Curious about the origin of differences in ΔH_{app}, and about whether a protein with two such well-defined subdomains is truly one cooperative unit of folding, we decided to investigate three strongly destabilizing mutations of the N-terminal region. These were a substitution of lysine for alanine at position 42 (A42K), and insertions of a single alanine into an α-helix at position 44 (S44[A]) or position 48 (K48[A]) (Heinz et al., 1993, 1994). All of the mutant proteins also had both of the two cysteines of the wild-type lysozyme mutated (C54T:C97A) (Nicholson et al., 1991), to prevent unwanted disulfide bond formation. It

Received for publication 14 May 1996 and in final form 3 July 1996.

Address reprint requests to Dr. Peter L. Privalov, Biology Department, Johns Hopkins University, 3400 N. Charles St., Baltimore, MD 21218. Tel.: 410-516-6037; Fax: 410-516-5213; E-mail: jhc@kelvin.bio.jhu.edu.

*This paper is dedicated to Serge Timasheff on the occasion of his 70th birthday.

0006-3495/96/10/1994/08 $2.00

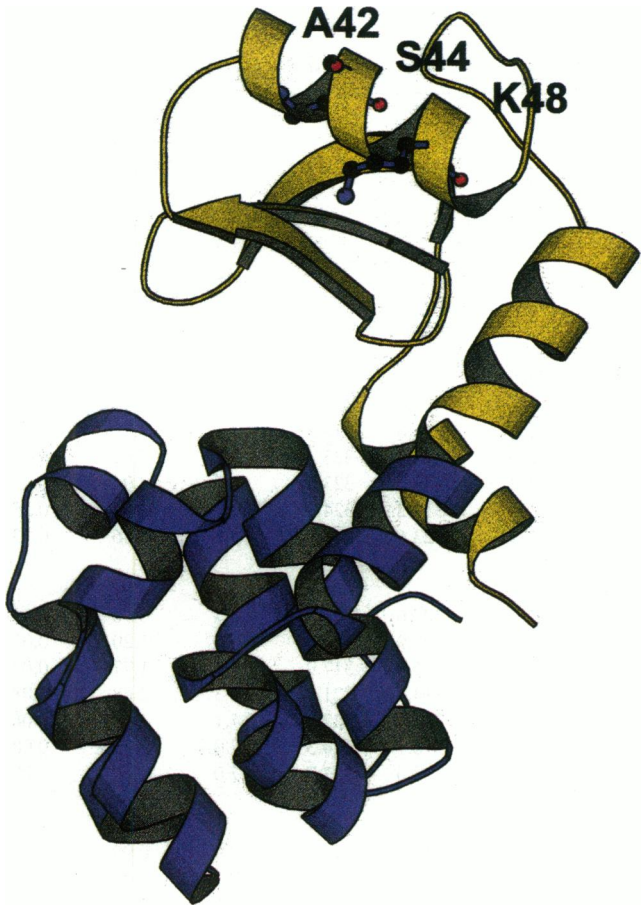

FIGURE 1 A ribbon drawing of the structure of wild-type T4 lysozyme (Bell et al., 1991), drawn using the program MOLSCRIPT (Kraulis, 1991) with coordinates from the Brookhaven Protein Data Bank (3zm.pdb). Residues 42, 44, and 48 are shown in a ball-and-stick representation. Residues 1–70 are shown in yellow and the remainder in blue, to highlight the N- and C-terminal subdomains.

is this cysteine-less pseudo-WT lysozyme that is used as a reference for this study.

MATERIALS AND METHODS

Protein purification

Proteins were purified from overproducing bacteria supplied by the laboratory of Dr. Brian Matthews, using the method of Poteete et al. (1991), except that cell lysis was achieved by repeated cycles of freeze-thawing, and the SP-Sephadex column step was replaced by FPLC over a Mono-S column. Protein concentrations were determined at room temperature using an absorbance value of 1.33 for a 1 mg ml^{-1} solution, calculated using the method of Gill and von Hippel (1989). Although some of the proteins studied may have been partially unfolded at room temperature, the tertiary structure of T4 lysozyme has a vanishingly small effect on its absorbance (Elwell and Schellman, 1975).

Differential scanning calorimetry, circular dichroism, and fluorescence measurements

Experiments were performed as described (Carra et al., 1994a), in 20 mM glycine-HCl buffer with 1 mM EDTA. The addition of NaCl to 100 mM resulted in aggregation after denaturation, and so extra salt was avoided. Protein concentrations used are given in Table 1. Over the limited twofold concentration range used, no significant concentration dependence of transition temperature or ΔH_{fit} was observed. Circular dichroism measurements were made at a protein concentration of 0.5 mg ml^{-1}, as described (Carra et al., 1994a). Tryptophan fluorescence measurements were made at a protein concentration of 0.1 mg ml^{-1} (Carra et al., 1994b).

Data analysis

Calorimetric and circular dichroism data were analyzed using models for either one endothermic transition (two-state model) or two sequential transitions (three-state model). Nonlinear least-squares fitting to these models was performed using equations input into the program NLREG (Phillip H. Sherrod, author).

The heat capacity of the unfolded state was fit to a quadratic function (Griko et al., 1995), whose first- and second-order coefficients (see Eq. 1) were obtained by calculating the heat capacity of fully unfolded lysozyme according to the method of Makhatadze and Privalov (1990). The constant term of this quadratic was allowed to vary as a parameter of the fitting. The heat capacity of the native state was fit to a linear function. The heat capacity of the unfolded state (C_{pU}) as a function of temperature (T, in Kelvin) is then

$$C_{pU} = -6.65 \times 10^{-4} * T^2 + 0.506 * T + A, \quad (1)$$

where A is a constant term adjusted in fitting. Other parameters varied in fitting were the transition temperature T_t, defined as the temperature where ΔG equals zero, and the enthalpy change ΔH_{fit} at T_t. ΔC_p was taken as a function of temperature from the difference in heat capacities of the unfolded and native states.

The excess heat capacity $\langle C_p \rangle$ due to the endotherm of a monomeric protein unfolding in a two-state process is given by the following (Freire, 1994, 1995):

$$\langle C_p \rangle = \frac{\Delta H^2}{(R * T^2)} * \frac{K}{(1+K)^2} \quad (2)$$

$$\Delta H = \Delta H_{fit} + \int_{Tt}^{T} \Delta C_p \, dT \quad (3)$$

$$\Delta S = \frac{\Delta H_{fit}}{T_t} + \int_{Tt}^{T} \Delta C_p \, d \ln T \quad (4)$$

$$\Delta G = \Delta H - T * \Delta S \quad (5)$$

$$K = \exp\left(\frac{-\Delta G}{R * T}\right). \quad (6)$$

K is the equilibrium constant of unfolding, ΔG is the Gibbs free energy change, ΔS is the entropy change, and ΔH is the enthalpy change, as functions of temperature. R is the gas constant (8.3145×10^{-3} kJ K^{-1} mol^{-1}). The partition function Q of the system (Privalov and Potekhin, 1986; Biltonen and Freire, 1978) in this case is simply

$$Q = 1 + K. \quad (7)$$

The fractional population of the native (F_N) and unfolded (F_U) states, as functions of temperature, can then be easily found:

$$F_N = \frac{1}{Q} \quad (8)$$

TABLE 1 Calorimetric results on T4 lysozyme mutants

pH	[Prot]*	2 st.# T_t	2 st.§ ΔH_{fit}	ΔH_{cal}	$\Delta H_{fit}/\Delta H_{cal}$¶	3 st. ΔH_{fit1}**	3 st. ΔH_{fit2}##	3 st. T_{t1}§§	3 st. T_{t2}¶¶	ΔC_p‖‖	2 st. σ^2***	3 st. σ^2###
					Pseudo-WT							
2.40	1.01	314.7	432	431	1.00					7.1	0.14	
2.60	0.98	318.6	469	468	1.00					7.7	0.25	
2.80	1.00	322.8	505	503	1.00					8.0	0.31	
3.00	0.89	327.1	534	533	1.00					6.1	0.58	
3.30	0.93	332.4	563	561	1.00					5.7	0.56	
3.50	0.86	335.1	572	571	1.00					9.8	0.39	
3.70	1.18	337.6	582	581	1.00					9.7	0.59	
					S44[A]							
3.00	0.99	311.4	267	302	0.88	108	225	305.1	311.7	6.7	1.14	0.12
3.20	1.00	317.1	305	373	0.82	160	222	314.5	317.5	2.7	3.36	0.23
3.30	1.10	318.1	307	376	0.82	129	251	312.8	318.5	7.1	2.75	0.09
3.60	0.997	322.8	324	400	0.81	148	259	318.5	323.3	7.1	3.61	0.12
3.70	0.565	323.9	325	378	0.86	120	271	318.6	323.8	5.5	2.04	0.23
3.70	1.11	323.9	322	379	0.85	118	274	317.2	324.2	10.5	2.93	0.25
4.00	1.03	327.3	356	442	0.80	170	279	323.6	327.9	7.1	4.86	0.13
					A42K							
3.00	1.15	311.8	274	301	0.91	102	219	307.6	311.3	6.7	0.76	0.12
3.20	1.16	316.1	298	331	0.90	107	255	308.9	316.1	6.5	1.20	0.05
3.30	1.16	317.9	307	354	0.87	120	252	312.8	317.9	6.7	1.77	0.07
3.50	1.16	320.9	319	383	0.83	123	269	314.4	321.1	8.3	2.68	0.08
3.60	1.16	323.1	321	372	0.86	109	271	317.3	322.9	7.1	1.71	0.06
3.70	1.17	324.4	336	409	0.82	123	278	318.7	324.3	7.0	2.86	0.08
4.00	1.10	327.4	355	440	0.81	158	280	323.6	327.7	7.0	4.55	0.08
					K48[A]							
3.00	0.624	314.6	364	390	0.93	187	216	317.7	311.9	7.9	0.99	0.26
3.50	0.659	322.9	391	436	0.90	170	267	324.6	321.1	8.2	1.72	0.14
4.00	0.641	327.6	386	430	0.90	173	271	328.2	326.4	7.3	1.49	0.17

*The protein concentration used in a DSC experiment, in mg ml^{-1}.
#Transition temperature T_t derived from fitting to a two-state model. Error is ±0.5 K.
§The fitted enthalpy change (ΔH_{fit}) from applying the two-state model to calorimetric data, in kJ mol^{-1}. Errors on ΔH values are ±10%.
¶The calorimetrically measured total enthalpy change (ΔH_{cal}) obtained using the two-state model, in kJ mol^{-1}.
‖The ratio of ΔH_{fit} to ΔH_{cal}, for the two-state model.
**The fitted enthalpy change (ΔH_{fit1}) in kJ mol^{-1} for the first transition of a three-state process.
##The same as the previous footnote, for the second transition (ΔH_{fit2}).
§§Transition temperature T_{t1} for the first endotherm of a three-state process.
¶¶T_{t2} for the second endotherm of a three-state process.
‖‖The total ΔC_p in kJ K^{-1} mol^{-1} at the two-state T_t.
***The variance σ^2 in kJ K^{-1} mol^{-1} of the fitted heat capacity function for the two-state model.
###The same for the three-state model.

$$F_U = \frac{K}{Q}. \tag{9}$$

The experimental data for each curve were fit to the following function C_p, which comprises all of the components of the heat capacity:

$$C_p = F_N * C_{pN} + F_U * C_{pU} + \langle C_p \rangle. \tag{10}$$

The calorimetric enthalpy change ΔH_{cal} is obtained simply by numerically integrating the experimental heat capacity data over the temperature range of the transition, while subtracting the terms $F_N * C_{pN}$ and $F_U * C_{pU}$, which describe the proportional contributions to C_p of the native and unfolded states in Eq. 10.

For the case of the three-state model, two sequential transitions are considered, from the native state (N) to an intermediate state (I), and from (I) to the unfolded state (U). In this case, the partition function Q is given as

$$Q = 1 + K_1 + K_1 * K_2 \tag{11}$$

$$F_N = \frac{1}{Q} \tag{12}$$

$$F_I = \frac{K_1}{Q} \tag{13}$$

$$F_U = \frac{K_1 * K_2}{Q}. \tag{14}$$

F_I is the fractional population of the intermediate state. K_1 and K_2 are the equilibrium constants of the first and second transitions, respectively, and are obtained from ΔG_1, ΔG_2, ΔH_{fit1}, ΔH_{fit2}, T_{t1}, and T_{t2}, as above. The heat capacity changes of the first (ΔC_{p1}) and second (ΔC_{p2}) transitions

were assumed to be proportional to ΔH_{fit1} and ΔH_{fit2}, and were obtained from the total ΔC_P as follows:

$$\Delta C_{p1} = \frac{\Delta H_{fit1}}{(\Delta H_{fit1} + \Delta H_{fit2})} * \Delta C_p \quad (15)$$

$$\Delta C_{p2} = \Delta C_p - \Delta C_{p1} \quad (16)$$

$$C_{pI} = C_{pN} + \Delta C_{p1}. \quad (17)$$

Our analytical approach is very similar to that of Griko et al. (1995), except that equations for a more specific case are used, and the shape of the unfolded state heat capacity was determined from the amino acid composition of the protein. For the three-state case, the excess heat capacities of the first ($\langle C_{P1} \rangle$) and second ($\langle C_{P2} \rangle$) transitions were derived from the excess enthalpy function ($\langle H \rangle$) as follows:

$$\langle H \rangle = \Delta H_{fit1} * (F_I + F_U) + \Delta H_{fit2} * F_U \quad (18)$$

$$\langle C_{P1} \rangle = \frac{(\Delta H_{fit1} * F_N * \langle H \rangle)}{(R * T^2)} \quad (19)$$

$$\langle C_{P2} \rangle = \frac{(\Delta H_{fit2} * F_U) * (\Delta H_{fit1} + \Delta H_{fit2} - \langle H \rangle)}{(R * T^2)}. \quad (20)$$

The function C_P to which the data are fit in the three-state case is then

$$C_p = F_N * C_{pN} + F_U * C_{pU} + F_I * C_{pI} + \langle C_{p1} \rangle + \langle C_{p2} \rangle. \quad (21)$$

Because the two-state model presupposes the existence of only two states, the fitted enthalpy ΔH_{fit} is analogous to the van't Hoff enthalpy, which relies on the same assumption and can be calculated from calorimetric data using this equation:

$$\Delta H_{vH} = \frac{4RT^2_m \langle C_p \rangle_{T_m}}{\Delta H_{cal}}. \quad (22)$$

For circular dichroism data, the ellipticity Θ was fit to the following equations for the two-state (23) and three-state (24) cases:

$$\Theta = F_N * \Theta_N + F_U * \Theta_U \quad (23)$$

$$\Theta = F_N * \Theta_N + F_I * \Theta_I + F_U * \Theta_U. \quad (24)$$

Θ_N, Θ_I, and Θ_U are the ellipticities of the native, intermediate, and unfolded states, respectively, which are assumed to be linear functions of temperature.

RESULTS

Although the x-ray crystal structure of the pseudo-WT lysozyme has been determined (Nicholson et al., 1991), the exact structures of the mutant proteins that we have chosen to study are unknown, because of their reluctance to crystallize (Heinz et al., 1993, 1994). The far-UV CD spectra of these mutant proteins are only slightly different from that of the pseudo-WT protein at pH 3.0 and 15°C (data not shown), indicating that the native-state secondary structure content of the mutants is largely or completely intact. The fluorescence spectra of the three tryptophans at positions 130, 138, and 158 in the C-terminal lobe are unaffected by the mutations, which is evidence for the retention of native structure in that region (data not shown). The peaks of the near-UV CD spectra of the mutants in the native state are decreased by about 20–25% relative to the pseudo-WT protein (data not shown), which may reflect some disordering of aromatic side chains due to packing defects in the N-terminal lobe.

Fig. 2 shows the results of differential scanning calorimetry on the pseudo-WT and S44[A] proteins. The melting temperature for the pseudo-WT protein was varied by changing pH in the range of 2.8 to 3.7. Above pH 4.0, aggregation occurred after denaturation. Within the pH range used, all melting curves were more than 90% reproducible upon reheating, if the first melt was stopped at 80°C, indicating that the reactions are reversible. An average ΔC_p value of 7.7 kJ K^{-1} mol^{-1} was found by analyzing the individual curves of the pseudo-WT protein, which is in reasonable agreement with the value of 6.5 kJ K^{-1} mol^{-1} estimated by fitting a line to the temperature dependence of ΔH_{cal} (Table 1).

The differential scanning calorimetry (DSC) data for the pseudo-WT and mutant proteins were first fit to a model of a two-state transition between the native and unfolded forms (Table 1, Materials and Methods). The transition temperature, as approximated by this analysis, is almost the same for the S44[A] mutant protein at pH 4.0 and the pseudo-WT protein at pH 3.0 (Table 1). This allows direct comparison of their heat capacity functions during melting (Fig. 2). The peak for the pseudo-WT protein is much sharper than that of the mutant protein. The sharpness of the peak is reflected in the value of the fitted enthalpy changes in Table 1 (ΔH_{fit}). As ΔH_{fit} was determined assuming a two-state process, it is analogous to the van't Hoff or apparent enthalpy change of unfolding. The calorimetric enthalpy change (ΔH_{cal}) is de-

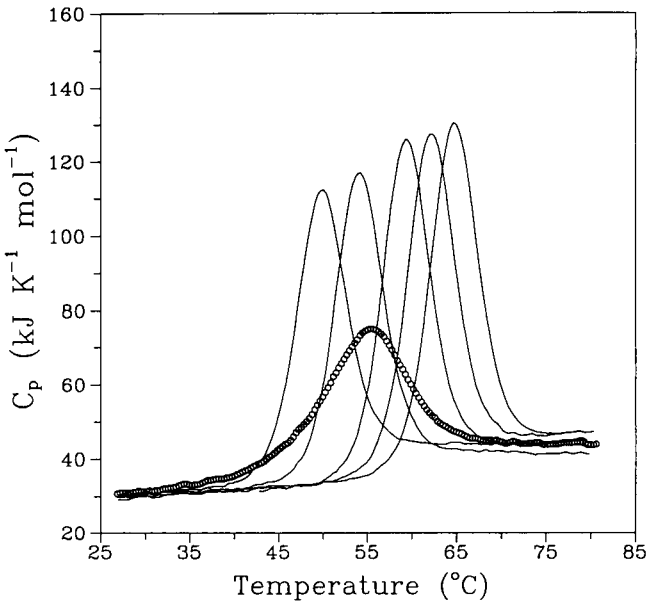

FIGURE 2 DSC results on the pseudo-WT T4 lysozyme (——) at pH values of 2.8, 3.0, 3.3, 3.5, and 3.7, in order of increasing denaturation temperature. ○, Data for the S44[A] mutant protein at pH 4.0.

termined by integrating the excess heat capacity of the endotherm (see Materials and Methods) and is the true total enthalpy change of the process.

The ratio of ΔH_{fit} to ΔH_{cal} is an indicator of the degree of cooperativity of unfolding. Values for this ratio of less than 1 indicate reduced cooperativity, whereas values greater than 1 would point toward other complexities, such as irreversibility of unfolding or multimolecular reactions. The ΔH_{fit}-to-ΔH_{cal} ratios of the mutant proteins are significantly less than 1 (Table 1), indicating reduced cooperativity. Reversibility was verified by cooling and rescanning the samples after heating.

The observation of reduced cooperativity for the mutants suggested that fitting to a three-state model, including a discrete intermediate state, was necessary. Fitting to a model of two sequential transitions was performed. The results are shown in Fig. 3 *A* for the S44[A] protein at pH 4.0. The excess heat capacity due to each transition can be seen, as well as their sum, the experimental data, and the extrapolated heat capacities of the native and unfolded states. The enthalpy change of the second transition is greater (Table 1), being 62% of the total. The fitted transition temperature T_{t1} for the first endotherm is less than that of the second endotherm by 4.3°C. Because the first transition is occurring at low temperatures, its endotherm contributes to the early part of the heat capacity curve. The slope of the heat capacity of the native state of the mutants was therefore assigned, using a constant value of 0.184 kJ K^{-2} mol^{-1} derived from the well-defined native-state heat capacity of the pseudo-WT protein (Fig. 2), for which this endotherm is not observed. The intercept of the native state heat capacity was constrained as necessary to fit the early portion of the curve well.

For the data at the lowest pH, 3.0, the mutant proteins were not completely native, even at low temperatures; thus these points are not as accurate as at higher pH values. Herein we will therefore mostly use the data at pH 4.0 for consideration of the mutant proteins.

For the pseudo-WT protein, the two-state model provides a good fit of the DSC data. However, it provides only a poor fit for the mutants, as can be seen in Fig. 3 *B*. The low-temperature portion of the excess heat capacity is neglected badly, and T_t is visibly off the mark. Allowing the slope of the native-state heat capacity to float freely resulted in poor fits, with the early part of the fitted heat capacity function diverging far from the experimental data. The variance of fit of the two-state and three-state models is given in Table 1, where it can be seen that for the mutant proteins the three-state model gives a much lower variance. Thus, use of the three-state model is necessary to achieve an accurate description of the unfolding process. From this analysis, the population of native, intermediate, and unfolded states can be calculated as a function of temperature (Fig. 4). For the case shown of the S44[A] mutant at pH 4.0, the intermediate state accumulates to a maximum of approximately 46% of the population of molecules. A three-state independent model also fit the data better than the two-state model, but

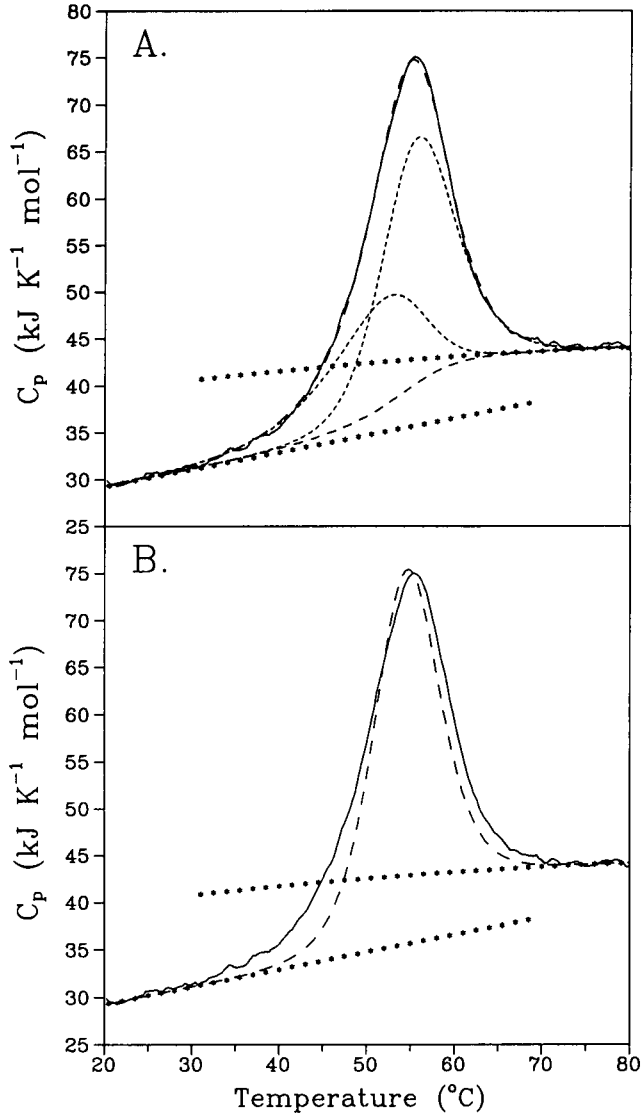

FIGURE 3 A. The heat capacity function of S44[A] protein at pH 4.0, fitted to a three-state model of two sequential transitions. ——, Experimental result; – – –, sum of fitted curves; - - -, fitted transitions; ***, assigned heat capacities of the native and unfolded states. (*B*) The same, except using a two-state model with one transition.

not as well as the sequential model, having a variance of 0.41 compared to 0.13 for this case. The sequential model was therefore preferred.

Reducing the protein concentration by half produced no significant change in ΔH_{fit1} and ΔH_{fit2} for the S44[A] protein at pH 3.7 (Table 1), indicating that the intermediate state is not an aggregate, which would be disfavored by reducing protein concentration. Moreover, unfolding of a multimolecular species would yield a $\Delta H_{fit}/\Delta H_{cal}$ ratio of greater than 1, whereas a ratio of less than 1 was found.

Fluorescence from the protein's tryptophans proved to have too steep an intrinsic temperature dependence to be useful as a probe of unfolding (data not shown). However, melting of the proteins could be monitored by following

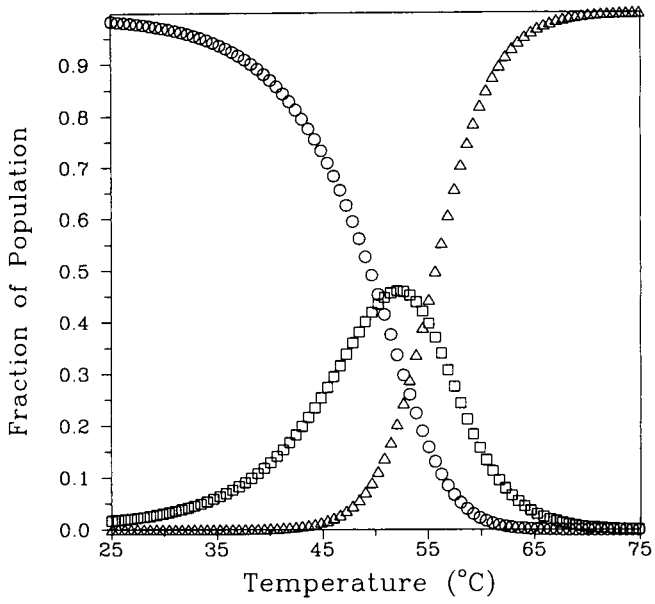

FIGURE 4 The populations of the native, intermediate, and unfolded states of S44[A] protein at pH 4.0. ○, Native; □, intermediate; △, unfolded states.

ellipticity at 222 nm (Fig. 5). The melting curve of the S44[A] mutant is much broader than that of the pseudo-WT protein and shows the presence of an early transition, which is consistent with the calorimetric result.

Fitting of the CD melting curves to a three-state model yielded values of 138 and 291 kJ mol^{-1} for ΔH_{fit1} and ΔH_{fit2}, respectively, for S44[A] protein at pH 4.0. These values are in reasonable agreement with the calorimetrically determined values of 170 and 279 kJ mol^{-1} (Table 1). In this case, we chose to assume that the ellipticity of the intermediate state is proportional to the fraction of α-helix (~40%) in the N-terminal subdomain, as divided in Fig. 1. However, because the intrinsic ellipticity of the intermediate state is essentially an unknown, detailed analysis of the CD data must be regarded as less reliable than the calorimetric analysis. The necessity of such assumptions often makes it impossible to assign a unique solution to the analysis of complex optically measured melting curves.

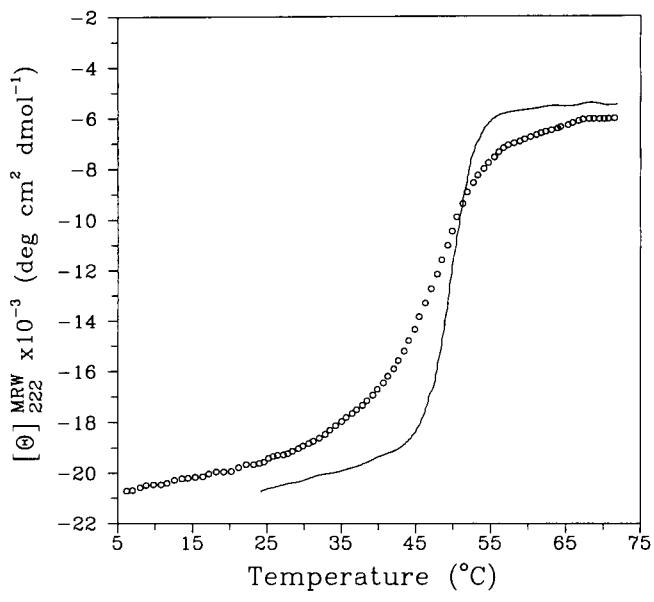

FIGURE 5 Melting of the pseudo-WT protein at pH 3.0 (——) and the S44[A] protein at pH 4.0 (○) followed by ellipticity at 222 nm.

DISCUSSION

Calorimetric investigation of these mutant T4 lysozyme proteins has revealed the presence of an intermediate state in unfolding. Three different strongly destabilizing mutations in the protein's N-terminal lobe yielded similar behaviors of unfolding through a discrete intermediate. The structural content of this form is uncertain. However, judging from the positions of the mutations involved, the intermediate is likely to have the N-terminal lobe partially or wholly unfolded and the C-terminal lobe intact. Both stages of unfolding involve some loss of ellipticity at 222 nm (Fig. 5); therefore the intermediate must have some but not all of the native state's helical content. The presence during unfolding of some population of multimolecular species cannot be excluded, but this would not correspond as well to the observed results as the considered model of a monomeric intermediate, and in any event would not invalidate our essential conclusion that an intermediate exists.

Evidence for an intermediate in unfolding of the wild-type T4 lysozyme during guanidine-HCl-induced denaturation has previously been obtained by Desmadril and Yon (1984), who also proposed that the C-terminal subdomain is more stable and folds faster than the N-terminal domain. Folding of the protein through a pathway of individual domains was further supported by the study of Anderson et al. (1990). Uverskii et al. (1993) observed a two-stage urea denaturation profile for a mutant having asparagine 101 changed to aspartate, consistent with the presence of a stable intermediate.

The total calorimetric enthalpy changes of unfolding the S44[A] and A42K mutant proteins as a function of temperature can be compared to those of the pseudo-WT protein in Fig. 6 *A*. At corresponding temperatures, there is a difference of approximately 90 kJ mol^{-1}, or roughly 15 to 20%, in ΔH_{cal} between the mutant and wild-type proteins. This difference is likely to be due to structural defects in packing of the unstable mutant proteins, which may also result in their diminished near-UV CD signals and difficulty in crystallization. The relatively large destabilization of these mutant proteins suggests that significant structural perturbations are present in the N-terminal region.

The difference in ΔH_{fit} for the two-state model between the mutants and pseudo-WT is even greater, as depicted in Fig. 6 *A*, being about 33% when considering S44[A] at pH 4.0 versus pseudo-WT at pH 3.0 (Table 1). The larger difference in ΔH_{fit} results from the lesser cooperativity of

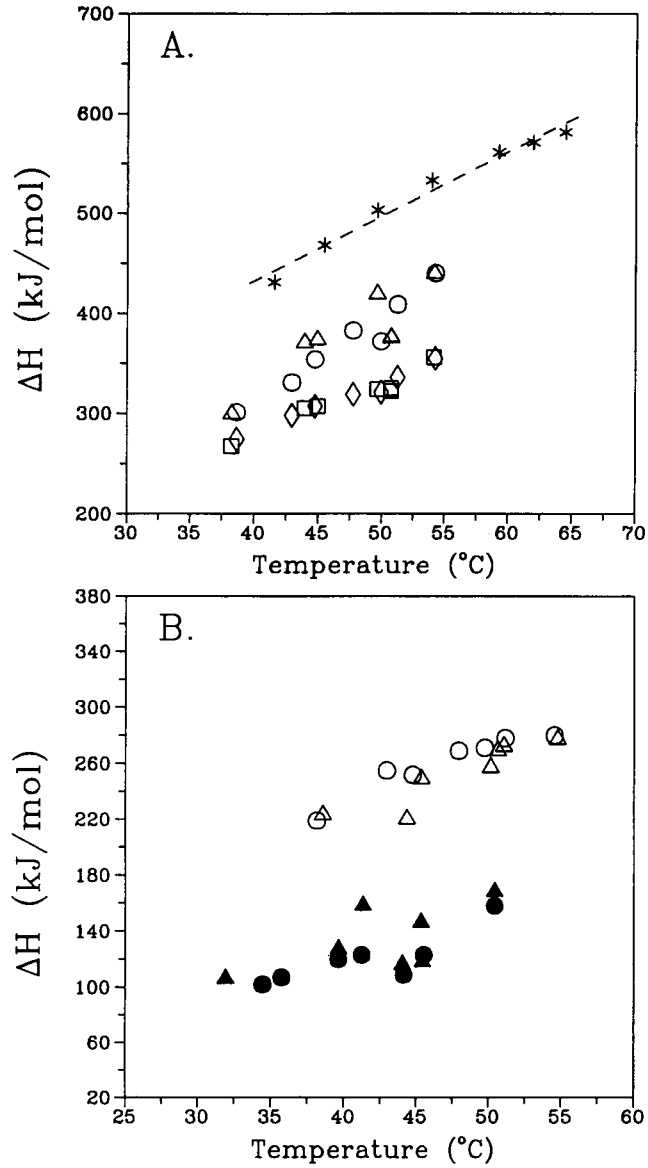

FIGURE 6 (*A*) ΔH_{cal} for the pseudo-WT (*), S44[A] (△), and A42K (○) proteins. Also shown are ΔH_{fit} from the two-state model for S44[A] (□) and A42K (◇). The temperature plotted is the transition temperature T_t, approximated using a two-state model for all cases, to facilitate comparison of two-state versus three-state processes. Data are from Table 1. (*B*) Fitted enthalpy changes for each transition of a three-state model, as applied for S44[A] (▲, ΔH_{fit1}, and △, ΔH_{fit2}) and A42K (●, ΔH_{fit1}, and ○, ΔH_{fit2}) proteins. T_t was determined more correctly from the three-state fitting.

folding of the mutant proteins. Because cooperativity is reduced for the mutants, the apparent enthalpy change represented by ΔH_{fit} underestimates the true enthalpy change.

Deviation from two-state behavior was earlier suggested as a possible explanation of the difference in apparent enthalpies for these mutants by Heinz et al. (1994). From this analysis, we can conclude that about half of the difference in apparent enthalpy changes between the mutants S44[A], K48[A], and A42K versus pseudo-WT is due to a reduction in cooperativity of unfolding.

In Fig. 6 *B* we have plotted the fitted enthalpy changes ΔH_{fit1} and ΔH_{fit2} for each transition of the mutants S44[A] and A42K. The temperature dependence of each of these parameters yields ΔC_{p1} and ΔC_{p2}, the heat capacity change of each transition, although these values cannot be assigned with great accuracy, because of uncertainties in the exact partition of enthalpies. ΔC_{p1} was found to be 2.5 and 2.8 kJ K^{-1} mol^{-1} for S44[A] and A42K proteins, respectively, whereas ΔC_{p2} was 3.9 and 3.6 kJ K^{-1} mol^{-1}. Their sum for each protein is 6.4 kJ K^{-1} mol^{-1}, close to the value of 7.2 kJ K^{-1} mol^{-1} calculated as an average of all the measured ΔC_p values of individual curves (Table 1).

A significant difference in the apparent van't Hoff enthalpy change between the wild-type and two other mutant T4 lysozymes was also reported by Elwell and Schellman (1977). Calorimetric investigations of the wild-type and some mutant lysozymes by Sturtevant and co-workers (Kitamura and Sturtevant, 1989; Connelly et al., 1991; Hu et al., 1992) found that the $\Delta H_{VH}/\Delta H_{cal}$ ratio decreased with higher pH, being approximately 0.8 at pH 2.84. Connelly et al. (1991) suggested that the change in this ratio may result from differences in pH sensitivity of subdomains in the bilobite protein. However, a three-state model was not explicitly applied to the data. Hu et al. (1992) did not find this pH sensitivity for the $\Delta H_{VH}/\Delta H_{cal}$ ratio of the C54T:C97A pseudo-WT protein. We did not find a pH dependence of this ratio for the pseudo-WT protein; however, there may be such a dependence for the A42K mutant (Table 1). The calorimetric report of Hu et al. found no evidence for intermediate states in several other mutants that were not as greatly destabilized as those studied herein.

A change in cooperativity also has critical significance for the calculation of the energetic parameters of folding. For a protein that unfolds through an three-state mechanism, one should calculate two individual terms for the Gibbs free energy changes of the first and second stages of the reaction (Carra and Privalov, 1996). The total ΔG of folding a protein is then the sum of these terms, and the change in total folding free energy due to mutation should be calculated from this sum. Fig. 7 shows the Gibbs free energy changes calculated for S44[A] mutant protein at pH 4.0, using either the two-state model and ΔH_{fit}, or the three-state model. The latter case yields two free energy changes, ΔG_1 and ΔG_2. The definition of the effective stability of the native state for this three-state mechanism of unfolding must be different from the case of a two-state mechanism and is represented by ΔG_1, the energy difference between the native and intermediate states. The effective stability of the mutant protein's native state is then lower than that calculated by assuming the absence of intermediates.

On the other hand, the total Gibbs free energy change of unfolding is the sum of ΔG_1 and ΔG_2. The difference between this sum and the free energy of folding the reference wild-type protein is the total free energy effect of the mutation on folding, and is much less than the effect that would be calculated if we had assumed a two-state model, as is commonly done in protein folding studies (Fig. 7).

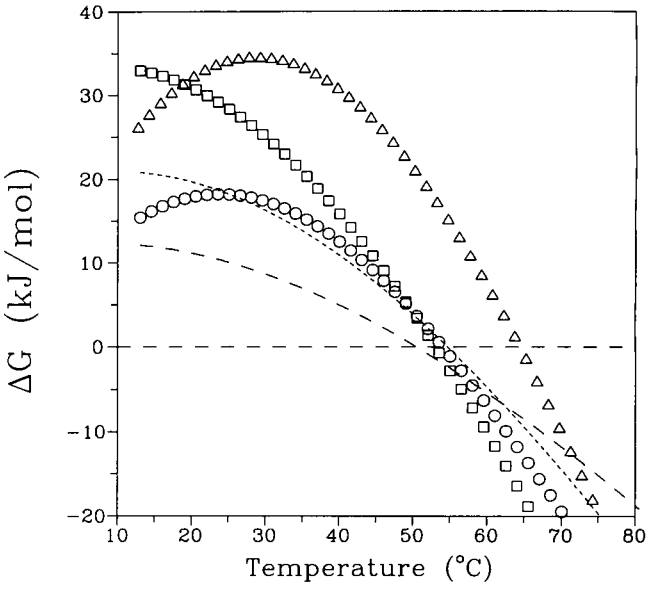

FIGURE 7 ΔG of unfolding S44[A] protein at pH 4.0 as a function of temperature, calculated as by Privalov (1979). Data are from Table 1. ○, Result calculated using the two-state model to obtain ΔH_{fit}, whereas the dashed lines show the free energy changes of the individual fitted transitions, ΔG_1 (– – –) and ΔG_2 (- - -), obtained from the three-state model. □, Sum of ΔG_1 and ΔG_2 for the mutant; △, ΔG for unfolding the pseudo-wild-type protein at pH 3.7, for purposes of comparison.

Accurate determination of the degree of cooperativity of unfolding is thus critical to understanding the energetic effects of mutations.

We are grateful to Dr. Brian Matthews and Joan Wozniak for the gift of strains overproducing the proteins used, and Kimberly Taylor for helpful advice.

This work was supported by National Institutes of Health grant GM 48036 and NSF grant MCB 9118687.

REFERENCES

Anderson, W. D., A. L. Fink, L. J. Perry, and R. Wetzel. 1990. Effect of an engineered disulfide bond on the folding of T4 lysozyme at low temperatures. *Biochemistry.* 29:3331–3337.

Bell, J. A., K. P. Wilson, X.-J. Zhang, H. R. Faber, H. Nicholson, and B. W. Matthews. 1991. Comparison of the crystal structure of bacteriophage T4 lysozyme at low, medium and high ionic strengths. *Proteins Struct. Funct. Genet.* 10:10–21.

Biltonen, R., and E. Freire. 1978. Thermodynamic characterization of conformational states of biological macromolecules using differential scanning calorimetry. *Crit. Rev. Biochem.* 5:85–124.

Carra, J., E. Anderson, and P. Privalov. 1994a. Thermodynamics of staphylococcal nuclease denaturation. I. The denatured state. *Protein Sci.* 3:944–951.

Carra, J., E. Anderson, and P. Privalov. 1994b. Thermodynamics of staphylococcal nuclease denaturation. II. The A-state. *Protein Sci.* 3:952–959.

Carra, J., E. Anderson, and P. Privalov. 1994c. Three-state thermodynamic analysis of the denaturation of staphylococcal nuclease mutants. *Biochemistry.* 33:10842–10850.

Carra, J., and P. Privalov. 1995. Energetics of denaturation and *m* values of staphylococcal nuclease mutants. *Biochemistry.* 34:2034–2041.

Carra, J., and P. Privalov. 1996. Thermodynamics of staphylococcal nuclease mutants: an intermediate state in protein folding. *FASEB J.* 10:67–74.

Connelly, P., L. Ghosaini, C-Q. Hu, S. Kitamura, A. Tanaka, and J. M. Sturtevant. 1991. A differential scanning calorimetric study of the thermal unfolding of seven mutant forms of phage T4 lysozyme. *Biochemistry.* 30:1887–1891.

Desmadril, M., and J. M. Yon. 1984. Evidence for intermediates during unfolding and refolding of a two-domain protein, phage T4 lysozyme: equilibrium and kinetic studies. *Biochemistry.* 23:11–19.

Elwell, M. L., and J. A. Schellman. 1975. Phage T4 lysozyme. Physical properties and reversible unfolding. *Biochim. Biophys. Acta.* 386: 309–323.

Elwell, M. L., and J. A. Schellman. 1977. I. Native properties and thermal stability of wild type and two mutant lysozymes. *Biochim. Biophys. Acta.* 494:367–383.

Freire, E. 1994. Statistical thermodynamic analysis of DSC data: structural deconvolution of the heat capacity function of proteins. *Methods Enzymol.* 240:502–568.

Freire, E. 1995. Thermodynamics of partly folded intermediates in proteins. *Annu. Rev. Biophys. Biomol. Struct.* 24:141–165.

Gill, S. C., and P. H. von Hippel. 1989. Calculation of protein extinction coefficients from amino acid sequence data. *Anal. Biochem.* 182: 319–326.

Griko, Y., E. Freire, G. Privalov, H. Van Dael, and P. Privalov. 1995. The unfolding thermodynamics c-type lysozymes: a calorimetric study of the heat denaturation of equine lysozyme. *J. Mol. Biol.* 252:447–459.

Heinz, D., W. Baase, F. W. Dahlquist, and B. W. Matthews. 1993. How amino-acid insertions are allowed in an α-helix of T4 lysozyme. *Nature.* 361:561–564.

Heinz, D., W. Baase, X-J. Zhang, M. Blaber, F. W. Dahlquist, and B. W. Matthews. 1994. Accommodation of amino acid insertions in an α-helix of T4 lysozyme. Structural and thermodynamic analysis. *J. Mol. Biol.* 236:869–886.

Hu, C-Q., S. Kitamura, A. Tanaka, and J. M. Sturtevant. 1992. Differential scanning calorimetric study of the thermal unfolding of mutant forms of phage T4 lysozyme. *Biochemistry.* 31:1643–1647.

Kitamura, S., and J. M. Sturtevant. 1989. A scanning calorimetric study of the thermal denaturation of the lysozyme of phage T4 and the Arg96 → His mutant form thereof. *Biochemistry.* 28:3788–3792.

Kraulis, P. 1991. MOLSCRIPT: a program to produce both detailed and schematic plots of protein structures. *J. Appl. Crystallogr.* 24:946–950.

Makhatadze, G., and P. Privalov. 1990. Heat-capacity of proteins. 2. Partial molar heat-capacity of the unfolded polypeptide-chain of proteins—protein unfolding effects. *J. Mol. Biol.* 213:385–391.

Nicholson, H., D. E. Anderson, S. Dao-pin, and B. W. Matthews. 1991. Analysis of the interaction between charged side-chains and the α-helix dipole using designed thermostable mutants of phage T4 lysozyme. *Biochemistry.* 30:9816–9828.

Poteete, A. R., S. Dao-Pin, H. Nicholson, and B. W. Matthews. 1991. Second-site revertants of an inactive T4 lysozyme mutant restore activity by restructuring the active site cleft. *Biochemistry.* 30:1425–1432.

Privalov, P. L. 1979. Stability of proteins. *Adv. Protein Chem.* 33:167–241.

Privalov, P. L. 1982. Stability of proteins. Proteins which do not present a single cooperative system. *Adv. Protein Chem.* 35:1–104.

Privalov, P. L. 1989. Thermodynamic problems of protein structure. *Annu. Rev. Biophys. Biophys. Chem.* 18:47–69.

Privalov, P. L., and S. A. Potekhin. 1986. Scanning microcalorimetry in studying temperature-induced changes in proteins. *Methods Enzymol.* 131:4–51.

Sturtevant, J. 1994. The thermodynamic effects of protein mutations. *Curr. Opin. Struct. Biol.* 4:69–78.

Uverskii, V. N., V. V. Leont'ev, and A. T. Gudkov. 1993. Effect of point amino acid replacements on the stability of phage T4 lysozyme. I. Asn101→Asp replacement. *Biophysics.* 38:619–622.